Dynamic Article Links

COMMUNICATION

Cyclization of RGD peptide sequences *via* the macrocyclic chelator DOTA for integrin imaging†

Guiyang Hao,[a] Xiankai Sun,*[a] Quyen N. Do,[a] Blanca Ocampo-García,[b] Andrea Vilchis-Juárez,[b] Guillermina Ferro-Flores[b] and Luis M. De León-Rodríguez*[c]

Two bicyclic compounds containing Arg-Gly-Asp (RGD) motifs (RGDf and RGD) were synthesized by cyclizing the peptide sequence across the macrocyclic ring of DOTA *via* two non-adjacent carboxylate pendent arms. The Lu^{3+} or Cu^{2+} complexes of these compounds, c(DOTA-RGDf) and c(DOTA-RGD), showed a metal dependent affinity towards integrin $\alpha_v\beta_3$ *in vitro* and the $^{177}Lu^{3+}$ or $^{64}Cu^{2+}$ labelled derivatives showed specific tumour uptake in MCF7 and U87MG tumour bearing mice.

The use of radiometal coordination complexes in nuclear medicine is important for the development of new receptor specific diagnostic and therapeutic agents.[1]

A typical approach used for developing specific agents involves the covalent attachment of a chelator, which should form a thermodynamically stable and kinetically inert complex with the radiometal, and a moiety (*e.g.* antibody, peptide, *etc.*) that specifically recognizes a given target. Usually, such attachment is done in a location where the binding affinity of the specific recognition unit to the target is not compromised by the conjugation. Among the chelators 1,4,7,10-tetraazacyclododecane-1,4,7,10-tetra acetic acid (DOTA) forms stable complexes with several radiometal ions (*e.g.* $^{68}Ga^{3+}$, $^{64}Cu^{2+}$ for positron emission tomography (PET), $^{111}In^{3+}$, $^{177}Lu^{3+}$ for single photon emission computed tomography (SPECT) and $^{90}Y^{3+}$ for radiotherapy). Integrins are biological targets of interest given their participation in angiogenesis and metastasis of tumours. Nine integrin subtypes have been implicated in one degree or another in angiogenesis,[2] and among these $\alpha_v\beta_3$, $\alpha_v\beta_5$ and $\alpha_5\beta_1$ have received the most attention given their key role in cancer progression.[3] Peptides containing the Arg-Gly-Asp (RGD) sequence

[a]*The University of Texas Southwestern Medical Center, 5323 Harry Hines Blvd, Dallas, TX 75390, USA. E-mail: xiankai.sun@utsouthwestern.edu; Fax: +1 214-645-2885; Tel: +1 214-645-5978*
[b]*Instituto Nacional de Investigaciones Nucleares, Carretera México-Toluca S/N, La Marquesa, Ocoyoacac, Estado de México, 52750, México. E-mail: guillermina.ferro@inin.gob.mx; FAx: +52 555-329-7306; Tel: +52 555-329-7200*
[c]*Universidad de Guanajuato, Cerro de la Venada S/N, Guanajuato, Gto. 36040, México. E-mail: lmdeleon@ugto.mx; Fax: +52 473-732-6252*
†Electronic supplementary information (ESI) available: Detailed synthesis and characterization data, molecular dynamics calculations, radiolabeling and full biodistribution data details. See DOI: 10.1039/c2dt31493b

are known to recognize integrins. Early studies showed that simple linear RGD containing peptides were active against several integrins but lacked selectivity. Later it was recognized that selectivity and affinity could be improved if the peptide's space conformation could be constrained to match the integrin bioactive conformation. The head to tail cyclization of short peptides came as a solution and cyclic pentapeptides containing the RGD motif such as c($^1R^2G^3D^4f^5X$) emerged as potent and selective integrin antagonists.[4] Structural–activity analysis of cyclic penta- and hexapeptides indicates that integrin selectivity depends on the separation and orientation of the Arg and Asp side chains and the kink around Gly. Thus for a cyclic pentapeptide to bind $\alpha_v\beta_3$ integrin over $\alpha_{IIb}\beta_3$ (platelet receptor) it is required that the Arg and Asp side chains are oriented almost parallel to one another on the same side of the ring resulting in a narrow opening of the kink.[5] It is also known that in cyclic pentapeptides the presence of D-Phe or D-Tyr is essential for activity while the amino acid in position 5 is not important. In fact, in most of the reported integrin imaging agents it is the fifth residue (usually a Lys) where DOTA and other moieties are conjugated to cyclic pentapeptides.[6–8]

Thinking of novel approaches to construct RGD peptides conjugated to DOTA with a constrained conformational space, in this work we propose the synthesis of bicyclic ligands consisting of DOTA and the RGD peptide sequence bridged through the non-adjacent 1,7 carboxylate arms of DOTA. The idea behind the bicyclic agents is that the bicyclic template may open a new conformational venue given the constraint imposed by the macrocycle to the peptide,[9] relative to the conventional RGD monocyclic systems, where DOTA is usually attached by one carboxylate group to the fifth residue of RGD pentapeptides, and where no constraint is imposed to the peptide by the macrocycle.[10–13] A plausible advantage of bicyclic systems relative to the conventional monocyclic design is that conformational variability and possibly binding affinity could be controlled not only by the peptide sequence but also by the metal ion of the complex. For instance, in DOTA lanthanide (Ln^{3+}) and Y^{3+} complexes the metal is coordinated by the four nitrogen and four carboxylate groups of DOTA in square antiprism (SAP) or twisted square antiprism geometries (TSAP).[14] On the other hand, in Cu^{2+} and Ga^{3+} DOTA complexes the metal ion is octahedrally coordinated to the four nitrogens and two (opposite) carboxylate arms, while the other two carboxyl groups are turned away from the metal.[15,16]
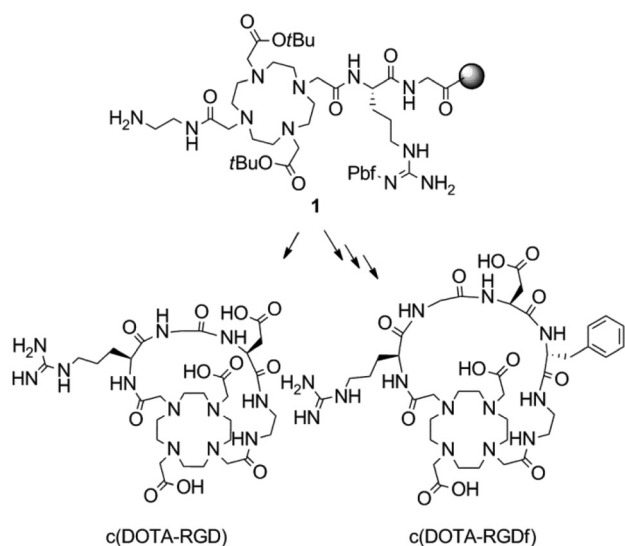
Scheme 1 Synthesis of the bicyclic systems.

Based on the structure–activity analysis of cyclic penta-peptides we first targeted the bicyclic DOTA bis-amide compounds shown in Scheme 1, c(DOTA-RGDf) and c(DOTA-RGD). In these two compounds the essential RGD sequence is present and an ethylenediamine linker was added as a moiety that would allow the head to tail cyclization of the final compound. The linker-macrocycle unit replaces the amino acid in position 5 of the cyclic pentapeptide as a way to minimize its influence on the activity of the final construct. Before we proceeded to the synthesis of these compounds we carried out Molecular Dynamics calculations as a way to determine if the bicyclic metal complexes will possibly fit into the binding pocket of $\alpha_v\beta_3$ by taking the crystal structure of the c(RGDf[NMe]V)-$\alpha_v\beta_3$ complex (ESI†) as a reference.[17] We found that most structural parameters considered important for RGD peptides to interact with $\alpha_v\beta_3$[18] were not significantly different when comparing c(DOTA-RGDf) and c(DOTA-RGD) with c(RGDf[NMe]V) (ESI, Table S1 and discussion in ESI†). This suggests that in principle the bicyclic derivatives might be able to bind $\alpha_v\beta_3$. We then proceeded with the synthesis of these derivatives using a solid phase-solution cyclization protocol (see ESI† for the complete synthetic procedure). Residue covalent attachment was accomplished following standard Fmoc solid phase peptide synthesis with Gly being attached first to an acid labile 2-chlorotrityl chloride resin. Arg was attached next followed by coupling of DOTAbis-*tert*-butyl ester[19] through one of the two free acetate groups. Ethylenediamine was reacted with the remaining free acetate of the peptidyl resin bound macrocycle to generate **1** (Scheme 1). To this intermediate we attached either D-Phe and Asp or only Asp that gave c(DOTA-RGDf) and c(DOTA-RGD), respectively, after the removal of the protected DOTA peptide from the resin followed by cyclization and removal of protecting groups in solution.

The *in vitro* affinity of the metal free bicyclic ligands and their Lu^{3+} complexes for integrin $\alpha_v\beta_3$ was determined by a competitive binding assay (ESI, Fig. S6†). The IC$_{50}$ values for c(DOTA-RGD) and its Lu^{3+} complex were approximately four times lower than for their RGDf counterparts. No significant IC$_{50}$ change was observed for both c(DOTA-RGD) and

Table 1 Integrin $\alpha_v\beta_3$ binding affinity. The IC$_{50}$ values were determined by the compound concentration required to displace 50% of a radioligand (^{177}Lu-DOTA-E-[c(RGDfK)]$_2$) bound to integrin $\alpha_v\beta_3$. Data are presented as IC$_{50}$ (nM) ± standard deviation (s.d.)

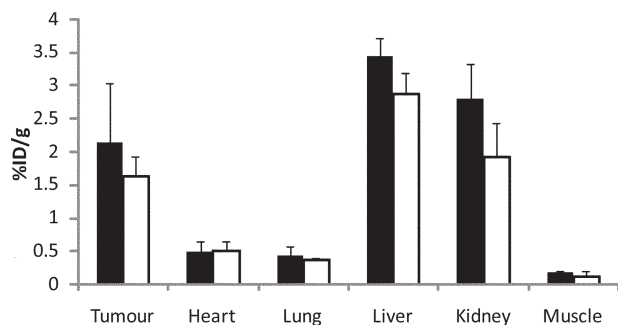| M	M-c(DOTA-RGD)	M-c(DOTA-RGDf)
No metal	4.7 ± 0.3	20.4 ± 3.5
Lu^{3+}	5.2 ± 0.5	17.0 ± 3.2
Cu^{2+}	11.5 ±1.0	13.5 ± 2.2
c(RGDfK)	6.7 ± 1.3	
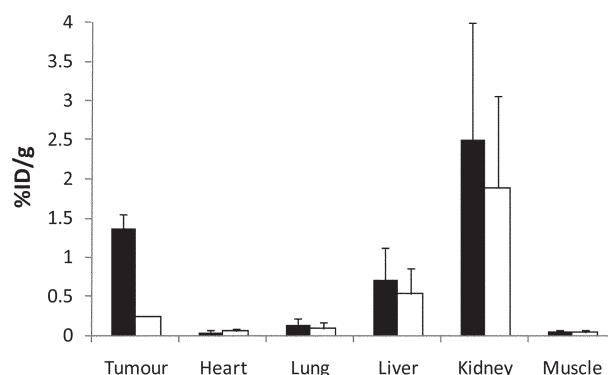
Fig. 1 Tissue distribution of ^{177}Lu-c(DOTA-RGD) in MCF7 tumour bearing mice at 3 h p.i. for unblocking (black bars) and blocking (white bars) experiments. Data are presented as %ID/g ± s.d. ($n = 3$).

c(DOTA-RGDf) when complexed with the Lu^{3+} complex (Table 1). Also the IC$_{50}$ values of c(DOTA-RGD) and its Lu^{3+} complex were found to be similar to that of the conventional pentapeptide c(RGDfK). Interestingly, the IC$_{50}$ of Cu-c(DOTA-RGD) was two-fold larger than the value determined for the free ligand or the corresponding Lu^{3+} complex, while the IC$_{50}$ of Cu-c(DOTA-RGDf) was ∼1.5 times lower than that of the free ligand. These $\alpha_v\beta_3$-integrin binding affinity differences as measured by the IC$_{50}$ values indicate that the metal has an important effect on the affinity of the compounds.

To determine if the bicyclic compounds can be applied for monitoring tumour integrin expression *in vivo* the ligands were labelled with ^{177}Lu^{3+}, a γ emitter ($t_{1/2}$ = 6.73 d; β^- (490 keV: 100%); γ (113 keV: 3%; 210 keV: 11%)). The radiolabeled derivatives were injected into MCF7 tumour bearing mice and their biodistribution was determined (ESI, Table S2†). The biodistribution data of ^{177}Lu-c(DOTA-RGD) are shown in Fig. 1 (black bars), where one can see that this agent was taken by the tumour and was eliminated *via* the kidneys. On the other hand, ^{177}Lu-c(DOTA-RGDf) showed a lower tumour uptake (ESI, Table S2†). The blockade study was also carried out by co-injecting c(RGDfK) with ^{177}Lu-c(DOTA-RGD) and this time tumour uptake decreased by 82% (Fig. 1 white bars).

Biodistribution studies were also carried out with ^{64}Cu^{2+}, a positron emitter ($t_{1/2}$ = 12.7 h; β^+ (653 keV: 17.4%); β^- (578 keV: 37%); EC (43%)), for PET-CT imaging (ESI, Table S3†) in U87MG tumour bearing mice. Quantitative PET data of ^{64}Cu-c(DOTA-RGDf) are shown in Fig. 2 (black bars) and PET images in Fig. 3, where one can see that this agent was taken by the tumour. ^{64}Cu-c(DOTA-RGDf) showed high liver uptake which was somehow expected since it is known that DOTA and

**Fig. 2** Quantitative PET data of ^{64}Cu-c(DOTA-RGDf) in U87MG tumour bearing mice at 4 h p.i for unblocking (black bars) and blocking (white bars) experiments. Data are presented as %ID/g ± s.d. ($n = 3$).
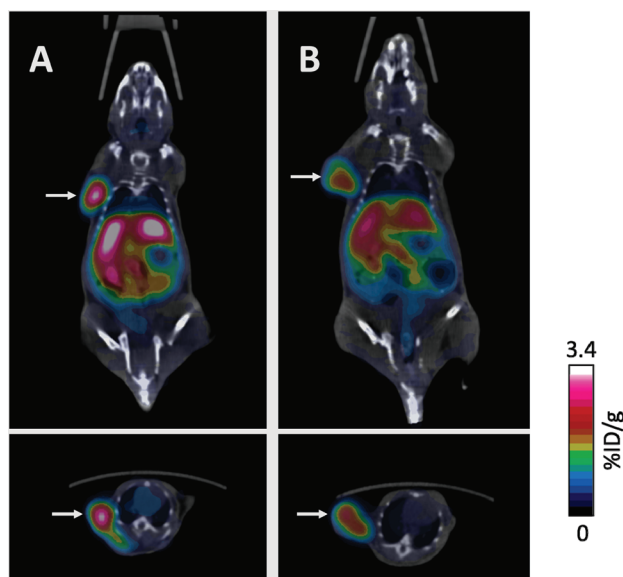
Fig. 3 Representative coronal and axial PET-CT images of ^{64}Cu-c(DOTA-RGDf) in U87MG tumour-bearing mice at 4 h p.i. ($n = 3$) without (A) and with (B) a blockade dose of c(RGDyK) (10 mg per kg of mouse weight). The white arrows indicate tumours.

particularly 1,4,7,10-tetraazacyclododecane-1,7-bis acetic acid 4,10-ethylene bicyclic Cu^{2+} complexes are not entirely kinetically inert.[20] On the other hand, ^{64}Cu-c(DOTA-RGD) showed lower tumour accumulation (ESI, Table S3†). Surprisingly, tumour uptake of ^{64}Cu-c(DOTA-RGDf) showed a small decrease in blocking experiments (Fig. 2 white bars) relative to the non-blocking data (Fig. 2 black bars). We also carried out experiments in U87MG xenograft mice using ^{64}Cu-DOTA-c(RGDyK), where DOTA is attached through an amide bond to the ε-amino group of lysine. In this case tumour accumulation decreased by 60% in blocking experiments when compared to non-blocking data (ESI, Table S3†). This indicates that the tumour uptake of ^{64}Cu-c(DOTA-RGDf) might not be exclusively mediated by integrin α$_v$β$_3$.

Tumour to organ uptake ratios (T/O) were calculated in order to determine how effectively the bicyclic metal complexes are targeting the tumours relative to background organs. Muscle and heart were chosen as the reference organs since the first one is a common background organ while in healthy mice the heart does not over-express α$_v$β$_3$ integrins and its uptake was considered as
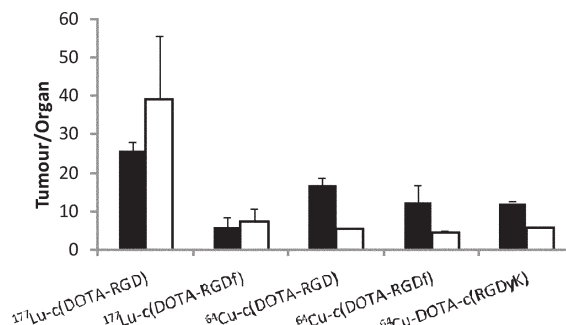
Fig. 4 Tumour/organ uptake ratios (black bars for muscle and white bars for heart) of the ^{177}Lu^{3+} complexes of c(DOTA-RGDf) and c(DOTA-RGD) in MCF7 tumour bearing mice (3 h p.i.) and the corresponding ^{64}Cu^{2+} complexes in U87MG tumour-bearing mice (4 h p.i.). The conventional integrin α$_v$β$_3$ PET probe, ^{64}Cu-DOTA-c(RGDyK), was included for comparison.

the blood activity kinetics. As shown in Fig. 4, T/O were much higher for ^{177}Lu-c(DOTA-RGD) than for ^{177}Lu-c(DOTA-RGDf) which agrees with the higher affinity of the former for α$_v$β$_3$. On the other hand T/O were slightly higher for the ^{64}Cu labelled c(DOTA-RGD) than for the c(DOTA-RGDf) complex which again concords with the affinities for α$_v$β$_3$ (Table 1).

The *in vitro* α$_v$β$_3$ binding affinity differences observed for the ^{177}Lu^{3+} and ^{64}Cu^{2+} complexes of the bicyclic systems presented herein could be attributed to the differences of their preferred coordination geometries. To gain further insight on the geometry of the Lu^{3+} bicyclic complexes in solution we prepared the corresponding Yb^{3+} complexes and acquired their ^{1}H NMR spectrum (Yb^{3+} and Lu^{3+} have similar ionic radius but the former induces large paramagnetic shifts which eases NMR spectra interpretation). Based on previous literature reports, the presence of methylene axial side protons from the macrocycle at *ca.* 90–110 ppm in the ^{1}H NMR spectra of both Yb^{3+} bicyclic complexes (ESI, Fig. S7 and S8† respectively) indicates that both complexes adopt a TSAP geometry in solution.[9] On the other hand, UV-Vis spectra of the Cu^{2+} bicyclic complexes (ESI, Fig. S9†) showed d–d transition bands with ε ∼ 40 L mol^{-1} cm^{-1} at 13 333 and 13 495 cm^{-1} for Cu-c(DOTA-RGDf) and Cu-c(DOTA-RGD) respectively. This indicates that these complexes exist in a distorted octahedral geometry in solution.[21]

Conclusions

In this work we presented the synthesis of bicyclic DOTA-RGD constructs as new chelate scaffolds for integrin targeting. The bicyclic metal complexes showed a metal dependent affinity towards α$_v$β$_3$ *in vitro*. Integrin imaging with ^{177}Lu^{3+} and ^{64}Cu^{2+} complexes of these bicyclic systems was demonstrated in two mouse xenograft models. Future efforts include the elucidation and optimization of the binding mode to integrins with these bicyclic moieties and their potential applications for specific imaging of integrins.

Acknowledgements

Notes and references

1 D. Josephs, J. Spicer and M. O'Doherty, *Target. Oncol.*, 2009, **4**, 151–168.
2 R. O. Hynes, *J. Thromb. Haemost.*, 2007, **5**, 32–40.
3 J. S. Desgrosellier and D. A. Cheresh, *Nat. Rev. Cancer*, 2010, **10**, 9–22.
4 C. Mas-Moruno, F. Rechenmacher and H. Kessler, *Anti-Cancer Agents Med. Chem.*, 2010, **10**, 753–768.
5 E. Lohof, E. Planker, C. Mang, F. Burkhart, M. A. Dechantsreiter, R. Haubner, H. J. Wester, M. Schwaiger, G. Hölzemann, S. L. Goodman and H. Kessler, *Angew. Chem., Int. Ed.*, 2000, **39**, 2761–2764.
6 S. Liu, *Mol. Pharm.*, 2006, **3**, 472–487.
7 W. Cai, G. Niu and X. Chen, *Curr. Pharm. Des.*, 2008, **14**, 2943–2973.
8 M. Luna-Gutierrez, G. Ferro-Flores, B. Ocampo-Garcia, N. Jimenez-Mancilla, E. Morales-Avila, L. De Leon-Rodriguez and K. Isaac-Olive, *J. Labelled Compd. Radiopharm.*, 2012, **55**, 140–148.
9 J. Vipond, M. Woods, P. Zhao, G. Tircso, J. Ren, S. G. Bott, D. Ogrin, G. E. Kiefer, Z. Kovacs and A. D. Sherry, *Inorg. Chem.*, 2007, **46**, 2584–2595.
10 X. Chen, Y. Hou, M. Tohme, R. Park, V. Khankaldyyan, I. Gonzales-Gomez, J. R. Bading, W. E. Laug and P. S. Conti, *J. Nucl. Med.*, 2004, **45**, 1776–1783.
11 M. Yoshimoto, K. Ogawa, K. Washiyama, N. Shikano, H. Mori, R. Amano and K. Kawai, *Int. J. Cancer*, 2008, **123**, 709–715.
12 C. Decristoforo, I. Hernandez Gonzalez, J. Carlsen, M. Rupprich, M. Huisman, I. Virgolini, H. J. Wester and R. Haubner, *Eur. J. Nucl. Med. Mol. Imaging*, 2008, **35**, 1507–1515.
13 X. Zhang, H. Liu, Z. Miao, R. Kimura, F. Fan and Z. Cheng, *Bioorg. Med. Chem. Lett.*, 2011, **21**, 3423–3426.
14 S. Aime, M. Botta, M. Fasano, M. P. M. Marques, C. F. G. C. Geraldes, D. Pubanz and A. E. Merbach, *Inorg. Chem.*, 1997, **36**, 2059–2068.
15 A. Riesen, M. Zehnder and T. A. Kaden, *J. Chem. Soc., Chem. Commun.*, 1985, 1336–1338.
16 N. A. Viola, R. S. Rarig Jr., W. Ouellette and R. P. Doyle, *Polyhedron*, 2006, **25**, 3457–3462.
17 J. P. Xiong, T. Stehle, R. Zhang, A. Joachimiak, M. Frech, S. L. Goodman and M. A. Arnaout, *Science*, 2002, **296**, 151–155.
18 D. Heckmann and H. Kessler, *Methods Enzymol.*, 2007, **426**, 463–503.
19 L. M. De Leon-Rodriguez, Z. Kovacs, A. C. Esqueda-Oliva and A. D. Miranda-Olvera, *Tetrahedron Lett.*, 2006, **47**, 6937–6940.
20 C. A. Boswell, X. Sun, W. Niu, G. R. Weisman, E. H. Wong, A. L. Rheingold and C. J. Anderson, *J. Med. Chem.*, 2004, **47**, 1465–1474.
21 C. F. G. C. Geraldes, M. P. M. Marques, B. De Castro and E. Pereira, *Eur. J. Inorg. Chem.*, 2000, 559–565.